

Giant Magnetoresistance in Multilayers with Noncollinear Magnetizations

S. Urazhdin,^{1,2} R. Lohmeier,² and W. P. Pratt Jr.²¹Department of Physics and Astronomy, Johns Hopkins University, Baltimore, MD, 21218²Department of Physics and Astronomy and Center for Fundamental Materials Research, Michigan State University, East Lansing, MI, 48824

We study the dependence of perpendicular-current magnetoresistance in magnetic multilayers on the angle between the magnetizations of the layers. This dependence varies with the thickness of one of the layers, and is different for multilayers with two and three magnetic layers. We derive a system of equations representing an extension of the two-current series resistor model, and show that the angular dependence of magnetoresistance gives information about the noncollinear spin-transport in ferromagnets.

PACS numbers: 72.25.Mk, 73.21.Ac, 75.47.De

The discoveries of giant magnetoresistance (GMR) [1] and spin-transfer [2] in ferromagnetic metallic multilayers greatly contributed to our understanding of the relation between magnetism, charge, and spin transport, and lead to important applications in memory devices and sensors. The spin-torque theory of spin-transfer relies on the absorption of the transverse spin-current at the magnetic interfaces in multilayers with noncollinear magnetizations, due to the averaging of spin-dependent electron reflection at the interfaces, and spin-precession inside the ferromagnets [3, 4, 5, 6, 7, 8, 9, 10, 11, 12]. Similarly, the disappearance of the transverse spin-current inside ferromagnets is predicted to affect the angular dependence of perpendicular-current (CPP) GMR in multilayers with noncollinear magnetizations (AGMR). Thus, AGMR is an important effect complementary to the spin-torque.

Theories of AGMR qualitatively agree with the available data [12, 13, 14, 15], but quantitative agreement has not yet been achieved. Due to the lack of systematic studies, it is also impossible to verify the predicted tendencies for the variation of AGMR with the multilayer parameters. Here, we present a systematic study of AGMR in multilayers with two and three magnetic layers, in which we varied the thickness of one of the layers. The dependence of AGMR on this thickness is different in the two studied structures. Our analysis shows that magnetic interfaces, transverse to magnetizations spin-currents in ferromagnets, and in some cases sample leads give contributions to AGMR. These findings are important for the understanding of spin-transport in ferromagnets and theories of spin-torque.

Our sample fabrication and measurement techniques were described elsewhere [16]. The structure of sample type A was Nb(150)Cu(20)FeMn(8)Py(6)Cu(10)Py(1.5-12)Cu(20)Nb(150), Py=Permalloy= $\text{Ni}_{84}\text{Fe}_{16}$ (Fig. 1). We label these samples A1.5, A3, A6, A12 by the thickness t_{Py} of the top Py layer. All thicknesses are in nanometers. Samples B1.5-12 had structure Nb(150)Cu(20)FeMn(5-12)Py(6)Cu(10)Py(1.5-12)Cu(10)Py(6)FeMn(5-12)Cu(20)Nb(150), and were labeled by the thickness of the middle Py layer. The

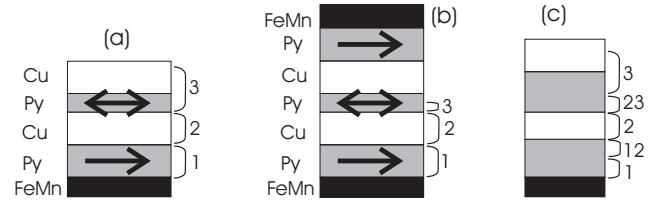


FIG. 1: (a,b) Schematics of samples A (a) and B (b), with layer compositions as labeled (thicknesses not to scale). Different sections of samples are labeled 1-3, as described in the text. (c) Schematic of the model incorporating finite transverse spin-current decay length.

bottom Py(6) in samples A, and the outer Py(6) layers in samples B were exchange-biased by annealing in magnetic field $H = 30$ Oe at 170 C. At least 2 samples of each type were measured with similar results.

Sample resistances R were measured with a SQUID voltmeter at 4.2 K in a CPP geometry. Fig. 2(a) shows an example of R vs. H curve for sample A12, measured with $H > 0$ along the pinning direction of the bottom Py layer. At large $H > 0$, magnetizations of both Py layers are parallel (P) to each other and H , giving low resistance R_P . As H decreased to small $H < 0$, the free layer switched to give antiparallel (AP) state with high resistance R_{AP} . The free layer coercive field H_c (half the width of its hysteresis) decreased from 30 Oe in samples A1.5 to 10 Oe in A12. The decrease of resistance to R_P at significantly larger $H < 0$ is due to switching of the pinned Py layer. We define the bias field H_b as H necessary to achieve $R = (R_P + R_{AP})/2$. In most samples, $|H_b| \approx 800$ Oe. Because $H_c \ll H_b$, we were able to rotate the free Py layer's magnetization, not significantly affecting the pinned one.

Fig. 2(b) shows examples of the AGMR measurements for samples A1.5 and A12, performed by rotating a fixed $H = 25 - 100$ Oe in the plane of the films. At angle $\theta = 0$, H is in the pinning direction of the bottom Py. There was no significant dependence of data on $25 - 100$ Oe in samples A3-A12. In samples A1.5, $H = 25$ Oe

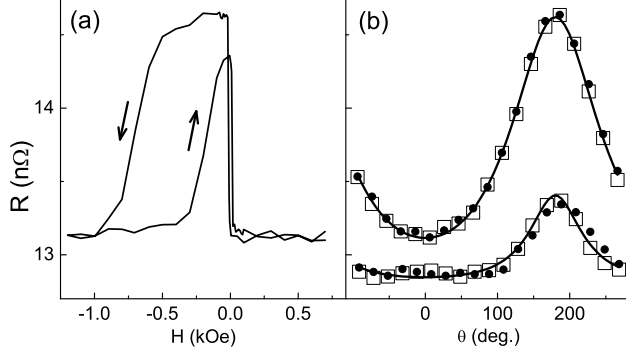


FIG. 2: (a) R vs. H in sample A12. (b) AGMR at $H = 25$ Oe (dots) and $H = 100$ Oe (squares) in samples A1.5 (bottom) and A12 (top). Solid lines are fits of the 100 Oe data with $\lambda = 7:7:0.6$ and $\lambda = 1:96:0.05$, respectively, as described in the text. For clarity, not all the measured points are shown, and the A1.5 data are offset by 0.2 n.

was insufficient to completely reorient the Py(1.5) layer due to its higher coercivity, but at $50 < H < 100$ Oe data were independent of H . Thus, we conclude that: a) our $H > 100$ Oe H_b does not significantly affect the magnetization of the pinned layer, b) Except for samples A1.5, $H = 25$ Oe was sufficient for monodomain rotation of the free layer.

Solid lines in Fig. 2 (b) are fits of the 100 Oe data with

$$R(\theta) = R_P + R \frac{1 - \cos^2(\theta/2)}{1 + \cos^2(\theta/2)}; \quad (1)$$

proposed by Giacomoni et al. [15], and later derived for symmetric spin-valves [4, 5, 6, 7, 8, 9, 10, 11]. In Eq. 1, $R = R_{AP} - R_P$, and λ is a fitting parameter. Eq. 1 gives good fit for all samples except for A1.5. In all three samples A1.5, the best fit did not completely reproduce the nearly constant data for $90^\circ < \theta < 90^\circ$. Because of the finite $\lambda = 0$ curvature of the fit, it was below the data at $\theta = 0^\circ$, and slightly above it around $\theta = 100^\circ$. Data for A1.5 in Fig. 3(b) show a weak rise around $\theta = 0^\circ$, similar to the uncertainty of the measurements.

Both $R(H)$ and AGMR data for samples B were qualitatively similar to those in Fig. 2. Figs. 3(a,b) summarize the A/R measurements (where A is the sample area) for samples A and B, and Figs. 3(c,d) show the χ values, extracted by fitting the AGMR data with Eq. 1. To reduce the uncertainty, χ obtained from 100 Oe and 50 Oe data were averaged for each point. At large t_{Py} , sample B is expected to behave similarly to two samples A connected in-series. Consistently, Fig. 3 shows that A/R for samples B12 is double that for samples A12, while χ s are close. At smaller t_{Py} , A/R in samples A decreases faster than half of that in samples B. In samples A,

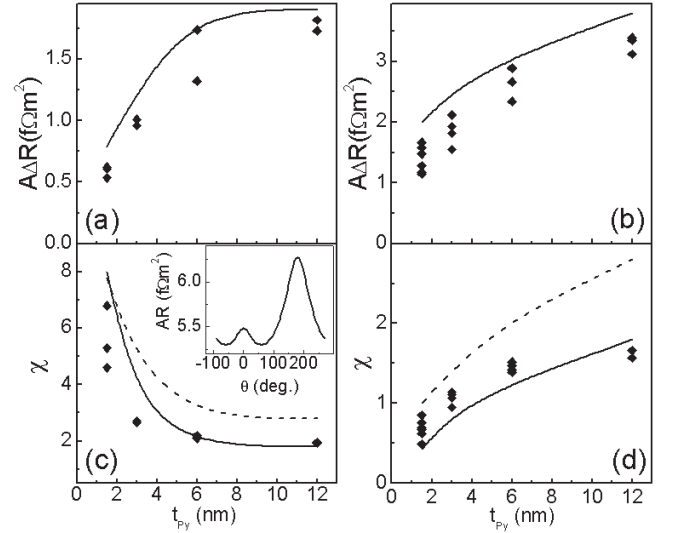


FIG. 3: (a) Measured (symbols) and calculated (line) A/R vs. t_{Py} for samples A. (b) Same as (a), for samples B. (c) χ from the fits of measured (symbols) and calculated (lines) AGMR with Eq. 1 for samples A. Solid line is calculated with correction for a finite $\lambda_L = 0.8$ nm, dashed line with $\lambda_L = 0$. Inset: calculated $R(\theta)$ for A1.5, as described in the text. (d) Same as (c), for samples B. All the lines are B-spline fits of the calculated points for $t_{Py} = 1.5; 3; 6; 12$ nm.

increases, while in samples B it decreases at smaller t_{Py} .

Several models have treated AGMR [4, 5, 6, 7, 8, 9, 10, 11, 12]. They predict the form Eq. 1 for symmetric spin-valves, but overestimate typically by a factor of two. Some theories predict a negligible length scale λ_L for the decay of the transverse spin-current in Py [4, 5]. Others correlate λ_L with the magnetic length $\lambda_m \approx 4$ nm in Py [7].

We develop an extension of the two current series resistor model [17] (2CSR) to AGMR, which contains much of the same physics as these other models, but allows us to gain qualitative insight into our results, analyze the effects of finite λ_L , and include the effect of the Nb sample leads, which we shall see give an important contribution to the measured dependencies.

In 2CSR, one separately considers two spin-current channels, same across the whole sample. For noncollinear magnetizations, two common spin-channels across the multilayer generally do not exist, so one needs to consider how the spin-channels are transformed across the multilayer. In samples A, we consider three parts of the multilayer (labeled 1-3 in Fig. 1(a)), separated by the Py/Cu interfaces 12 and 23. The outer limits of regions 1 and 3 are determined by the spin-diffusion, i.e. the GMR-active part of the multilayer. This additional constraint augments 2CSR and is essential for the following analysis. At each point of the multilayer, we define a matrix current $\hat{I} = \begin{pmatrix} I_1^{11} & I_1^{12} \\ I_1^{21} & I_1^{22} \end{pmatrix}$, which gives charge

current $I_c = \text{Tr} \hat{f}$ and projection of spin current on an arbitrary axis m , $I_s(m) = \hbar \text{Tr}(\hat{f}_m \hat{f}) = (2e) \cdot M$ matrix product of \hat{f} and the Pauli matrices \hat{f}_m is implied here. We assume that, due to averaging of spin-precession in the ferromagnets, the component of spin-current transverse to the Py magnetizations vanishes in regions 1 and 3 [3, 4, 5]. Later, we will discuss and modify this assumption. In region 1, the matrix current \hat{f}_1 is then diagonal in the frame set by the magnetization M_1 of the bottom Py layer, $\hat{f}_1 = \text{diag} \hat{f}_1^0$. Similarly, in region 3, $\hat{f}_3 = \text{diag} \hat{f}_3^0$. We use primed symbols for the frame set by the orientation of the top Py magnetization M_2 .

If spin- \uparrow scattering within regions 1-3 is neglected, \hat{f} is conserved separately across each region. However, only I_c and the spin-current projections on the corresponding Py magnetizations are conserved at the interfaces 12 and 23, therefore $\hat{f}_1 = \text{diag} \hat{f}_2$, $\hat{f}_3 = \text{diag} \hat{f}_2$. Here $\hat{f}^0 = \hat{U}^\dagger \hat{f} \hat{U}$, $\hat{U} = \begin{pmatrix} \cos(\theta/2) & \sin(\theta/2) \\ \sin(\theta/2) & \cos(\theta/2) \end{pmatrix}$ is the spin rotation matrix by angle θ between M_1 and M_2 .

We describe the local electron distributions by 2×2 spinor distribution matrices [8, 9]. Their diagonal elements in an arbitrary reference frame are given by the spin-up and spin-down electron densities, related to this frame. We neglect scattering in the Cu spacer between the Py layers, i.e. assume a position independent distribution in region 2. Finally, we introduce matrix resistances $\hat{R}_1 = \begin{pmatrix} 2R_1 & 0 \\ 0 & 1 + \frac{1}{R_1} \end{pmatrix}$, $\hat{R}_3 = \begin{pmatrix} 2R_3 \hat{U} & 0 \\ 0 & 1 + \frac{1}{R_3} \hat{U}^\dagger \end{pmatrix}$, $\hat{R}_{12} = \begin{pmatrix} 2R_{12} & 0 \\ 0 & 1 + \frac{1}{R_{12}} \end{pmatrix}$, and $\hat{R}_{23} = \hat{U} \hat{R}_{12} \hat{U}^\dagger$ (for identical interfaces 12 and 23), which connect matrix currents across regions 1 and 3, and interfaces 12 and 23, to the corresponding variations of the electron distributions. R , θ , and θ' are standard GMR notations [17].

The total voltage across the multilayer $\hat{V} = \begin{pmatrix} V & 0 \\ 0 & V \end{pmatrix}$ is the sum of electron distribution variations across regions 1 and 3, and interfaces 12 and 23,

$$\hat{V} = \hat{R}_1 \hat{f}_1 + (\hat{R}_{12} + \hat{R}_{23}) \hat{f}_2 + \hat{R}_3 \hat{f}_3 = \hat{R}_1 \text{diag}(\hat{f}_2^0) + (\hat{R}_{12} + \hat{R}_{23}) \hat{f}_2 + \hat{R}_3 \hat{U} \text{diag}(\hat{U}^\dagger \hat{f}_2^0 \hat{U}) \hat{U}^\dagger : (2)$$

Eq. 2 connects four unknown components of \hat{f}_2 to the voltage \hat{V} across the multilayer. The diagonal components of Eq. 2 reduce to 2CSR in the collinear limit. Once Eq. 2 is solved for \hat{f}_2 , the resistance of the multilayer is given by $R(\theta) = V / \text{Tr} \hat{f}_2$. We note that while Eq. 2 is written in the frame of M_1 , it can be transformed to an arbitrary reference frame.

For a symmetric bilayer, $R_1 = R_3$, $\theta = \theta'$, Eq. 2 is diagonal in the frame rotated halfway between M_1 and

M_2 . In this special case

$$R(\theta) = 2R_1 + 2R_{12} \frac{2 \cos^2(\theta/2) (R_1 + R_{12})^2}{R_{12} + R_1 \cos^2(\theta/2)} : (3)$$

This expression has the same form as Eq. 1, with $\theta = \theta'$, $R_1 = R_{12}$. As we noted above, R_1 and θ are determined by the condition that only the GMR-active part of the multilayer is included. In particular, in samples A12 $t_{Py} > l_{sf} = 5.5 \text{ nm}$, the spin-diffusion length in Py [18], so only the l_{sf} -thick parts of the Py layers should be included in regions 1 and 3. Thus, samples A12 are approximately symmetric, and can be described by Eq. 3. Similar arguments hold for samples B12, viewed as two samples A connected in series. We use the parameters established in CPP-GMR measurements [18], $AR_1 = l_{sf} \rho_{Py} = 1.4 \text{ fm}^2$, $\theta = \theta' = 0.7$, $AR_{12} = 0.5 \text{ fm}^2$, $\theta = 0.7$. We obtain $\theta = \theta' = 2.8$, larger than the measured $\theta = 2.0$ for A12, and $\theta = 1.6$ for B12.

Overestimation of θ is a general tendency of the AGMR theories. The physical transparency of Eq. 3 allows us to identify the possible origins of this discrepancy, and appropriately correct our analysis. We assumed above that transverse spin-current and the non-diagonal electron distribution components vanish in Py arbitrarily close to the Py/Cu interface. However, a sharp Py/Cu interface may be an unjustified idealization. If the onset of the bulk ferromagnetic Py properties occurs over a finite thickness, where Py and Cu are alloyed, it is also reasonable to expect that the transverse spin-current decays over a finite length l_t , nominally inside Py. Moreover, some theories predict a finite l_t even when an ideally sharp interface is assumed [7]. Regardless of the physical origin, we can phenomenologically include a finite l_t into our model by expanding the interfaces 12 and 23 into finite l_t -thick regions of Py (Fig. 1(c)), where spin-current is noncollinear to the magnetization. This correction decreases R_1 , and increases R_{12} , thus decreasing θ . $l_t = 0.8 \text{ nm}$ gives a good agreement of calculated θ with the data for samples A12 and B12.

AR is not affected by the finite l_t , irrelevant for the collinear transport. For t_{Py} comparable to l_t , the spin-torque should decrease due to incomplete transverse spin-transfer between electrons and magnetization. We note that in the published studies of spin-transfer (mostly with Co) the ferromagnet thicknesses were larger than l_t [19]. l_t in Co is likely even smaller than in Py due to its larger exchange splitting [7]. The circuit theory of spin-polarized transport and spin-transfer [6, 8, 9, 10] uses a mixing conductance parameter $g_{\#}$, characterizing spin-dependent scattering at the interfaces. Related to our model, $2g_{\#} = (R_{12})^{-1}$, thus it depends on l_t .

Giacomini et al. [15] obtained l_{12} for thick Py/Cu/Py spin-valves similar to our samples A12 or B12. Their smaller θ may be due to stronger alloying of the Py/Cu interfaces (giving larger l_t), caused by higher deposition rates and longer annealing time during pinning.

We modeled the dependence on t_{Py} by solving the general form of Eq. 2. The solution for asymmetric multilayers is similar to Eq. 1, but more complicated, and the denominator contains additional $\cos^4(\theta = 2)$ terms. We therefore give only numerical results for specific cases. One has $t_{Py} < l_{ef}$ in samples A1.5 and A3, so the GMR-active top part of the multilayer (region 3) must now include the entire top Py layer and the Py/Cu and Cu/Nb interfaces. Studies of Nb/Py and Nb/Cu/Py multilayers yield a large interface resistance $A R_{Py=Nb} \approx 3 \text{ f}\Omega^2$ [18], both with and without a Cu spacer between Py and Nb.

For samples A1.5, we added the full value of $R_{Py=Nb}$ to \hat{R}_3 , neglecting electron spin-flipping in Py(1.5). For A3, we added $0.5R_{Py=Nb}$ to approximately account for spin-flipping in Py(3), reducing the contribution of Py/Nb interface to GMR. Our model gives the same results for samples A1.2 and A6, but the difference in data is also small. The calculated $A R$ (Fig. 3(a), solid line) agrees well with the data. For samples A1.5, the calculated $R(\theta)$ significantly deviates from the form Eq. 1; Inset in Fig. 3(c) shows that it has maxima both at $\theta = 0$ and $\theta = 180^\circ$. A similar behavior is predicted for asymmetric spin-valves by the circuit theory [10]. Our calculation exaggerates a weak rise of data at $\theta = 0$ (Fig. 2(b)), but captures the overall experimental behavior. The quantitative discrepancy may be due to the neglected electron spin-flipping at the interfaces. In Fig. 3(c), solid line shows the calculated R , defined as the best fit with Eq. 1 to the calculated $R(\theta)$, using $l_t = 0.8 \text{ nm}$. The calculation using $l_t = 0$ (dashed line) gives a significantly worse agreement with data.

Samples B are symmetric with respect to the center of the middle Py layer. Therefore, current reversal does not change the electron distribution at that point for any magnetic orientation of the middle Py layer. Since the properly offset electron distribution is proportional to the current, we conclude that in the center of the middle Py layer the electron distribution is spin-independent. The model developed above for two magnetic layers can now be adopted to samples B with $t_{Py} < 2l_{ef}$, if we take half of the middle Py layer as region 3, as shown in Fig. 1(b). The top half of the sample simply doubles the resistance obtained from Eq. 2, not affecting θ . The results for $A R(t_{Py})$ and $R(t_{Py})$, with $l_t = 0.8 \text{ nm}$, are shown with solid lines in Figs. 3(b,d). The deviations from the form Eq. 1 were negligible for all samples B1.5-B12. Our model overestimates $A R$, but gives reasonable results for $R(t_{Py})$. Calculation assuming $l_t = 0$ (dashed line in Fig. 3(c)) gives a worse agreement with data.

Qualitatively, our results for $R(t_{Py})$ in both samples A and B can be understood with Eq. 3, derived for symmetric multilayers. In samples A, the activation of the highly resistive Py/Nb interface at smaller t_{Py} is equivalent to an increase of R_1 in Eq. 3, giving larger R . In samples B, smaller t_{Py} is equivalent to reduced R_1 in the

symmetric case, and thus smaller R .

In summary, we showed that the variation of GMR with angle between the magnetic layers (AGMR) depends on the thickness of one of the magnetic layers. The dependence is different in samples with two and three magnetic layers. To analyze the data, we developed an extension of the two current resistor model to multilayers with noncollinear magnetizations. Our analysis leads to the following conclusions: i) The deviation of AGMR from sinusoidal behavior is approximately given by the ratio of two quantities: a) the resistance of the GMR-active part of the multilayer excluding the noncollinear ferromagnetic interfaces, b) the resistance of these interfaces. The magnitude of this effect is not directly related to magnetic anisotropies and $A R$; ii) AGMR can be nonmonotonic in asymmetric spin-valves; iii) the transverse spin current penetration length l_t into ferromagnet can be extracted from AGMR. From our model, $l_t \approx 0.8 \text{ nm}$ for Py. l_t is an important parameter for the models of noncollinear spin transport in ferromagnets and spin-torque. The spin-torque should be reduced if the ferromagnet thickness is close to l_t .

We acknowledge helpful communications with M.D. Stiles, J. Bass, N.O. Birge, G.E.W. Bauer, support from the MSU CFMR, CSM, the MSU Keck Microfabrication facility, the NSF through Grants DMR-02-02476, 98-09688, and NSF-EU-00-98803.

-
- [1] M.N. Baibich et al, Phys. Rev. Lett. 61, 2472 (1988); G. Binasch et al, Phys. Rev. B 39, 2428 (1989).
 - [2] M. Tsui et al, Phys. Rev. Lett. 80, 4281 (1998); 81, 493(E) (1998).
 - [3] J. Slonczewski, J. Magn. Magn. Mat. 159, L1 (1996).
 - [4] J. Slonczewski, J. Magn. Magn. Mat. 247, 324 (2002).
 - [5] M.D. Stiles and A. Zangwill, J. Appl. Phys. 247, 324 (2002).
 - [6] A. Kovalev, A. Brataas, and G.E.W. Bauer, Phys. Rev. B 66, 224424 (2002).
 - [7] A. Shpiro, P.M. Levy, S. Zhang, Phys. Rev. B 67, 104430 (2003).
 - [8] G.E.W. Bauer et al, Phys. Rev. B 67, 094421 (2003).
 - [9] G.E.W. Bauer et al. in Advances in Solid State Physics ed. B. Kramer, Springer-Verlag, Berlin, 2003 (in press).
 - [10] J. Manschot, A. Brataas, G.E.W. Bauer, cond-mat/0309252 (2003).
 - [11] M.D. Stiles, unpublished.
 - [12] A. Vedyayev et al, Phys. Rev. B 55, 3728 (1997).
 - [13] P. Duguet et al, Phys. Rev. B 54, 1083 (1996).
 - [14] B.D.ieny et al, J. Appl. Phys. 79, 6370 (1996).
 - [15] L. G. iacomoni et al, unpublished.
 - [16] S.F. Lee et al, Phys. Rev. B 52, 15426 (1995) and ref. therein.
 - [17] J. Bass and W.P. Pratt, Jr., J. Magn. Magn. Mat. 200, 274 (1999).
 - [18] W.P. Pratt, Jr. et al, IEEE Trans. Magn. 33, 3505 (1997).
 - [19] F. J. Albert et al, Phys. Rev. Lett. 89, 226802 (2002).